



# A Bio-Inspired, Heavy-Metal-Free, Dual-Electrolyte Liquid Battery towards Sustainable Energy Storage

Yu Ding and Guihua Yu\*

**Abstract:** Wide-scale exploitation of renewable energy requires low-cost efficient energy storage devices. The use of metal-free, inexpensive redox-active organic materials represents a promising direction for environmental-friendly, cost-effective sustainable energy storage. To this end, a liquid battery is designed using hydroquinone ( $H_2BQ$ ) aqueous solution as catholyte and graphite in aprotic electrolyte as anode. The working potential can reach 3.4 V, with specific capacity of  $395 \text{ mAh g}^{-1}$  and stable capacity retention about 99.7% per cycle. Such high potential and capacity is achieved using only C, H and O atoms as building blocks for redox species, and the replacement of Li metal with graphite anode can circumvent potential safety issues. As  $H_2BQ$  can be extracted from biomass directly and its redox reaction mimics the bio-electrochemical process of quinones in nature, using such a bio-inspired organic compound in batteries enables access to greener and more sustainable energy-storage technology.

In modern society, energy and environmental issues are regarded as two grand challenges for human beings. Researchers are trying to use sustainable energy more efficiently without squandering natural resources or polluting the environment. Flow batteries using species in fluid forms, which allows an independent control on power and energy, can play a critical role in efficient storage of sustainable energy from often intermittent sources such as wind and solar power.<sup>[1]</sup> However, conventional flow batteries depend on redox-active metals and sometimes even precious-metal catalysts, which may inhibit wide-scale use limited by the material abundance and environmental issues. On the other hand, those redox reactions mainly take place in water, of which the potential window is limited to 1.23 V.<sup>[2]</sup> To break the glass ceiling of output potential, some groups turn their attention to a new energy storage system called lithium-redox battery.<sup>[3]</sup> The flowable catholyte makes it possible to scale up power and energy, and Li anode can promote the working potential. Nevertheless, most of current researches adopt either metal complexes or halogens as redox-active species, both of which are faced with cost and environmental

concerns.<sup>[3a,c]</sup> The direct use of Li anode also poses safety concerns.<sup>[4]</sup>

Quinones are well-represented organic molecules in biological electron-transfer processes, such as photosynthesis and ATP synthesis.<sup>[5]</sup> As one of the most important families of organic redox couples, their uses in the field of energy storage have been researched.<sup>[6]</sup> Despite that quinone-based solid-state battery using aprotic electrolyte is limited in long-term stability because of the dissolution of active materials,<sup>[7]</sup> the redox reaction of quinone in water has been proved to be highly stable in flow battery applications.<sup>[8]</sup> Some groups already exploited quinones as electroactive species in flow batteries showing expected performance.<sup>[9]</sup> Nevertheless, wider utilization of quinones is still faced with limitations. It is anticipated to build the battery with performance comparable with current technologies. In the meantime small molecules without complex synthesis method are preferred so as to increase specific capacity and lower the cost. To meet those requirements, we turned our attention to biomass-derived quinone molecules, and we designed the battery with  $Li^+$  as mediators to break the potential ceiling of 1.23 V in water using proton mediator.

Here we propose directly using hydroquinone ( $H_2BQ$ ) in water as catholyte for liquid battery. The chemical structure of  $H_2BQ$  features two hydroxyl groups bonded to a benzene ring in the *para* position. Different from its *ortho* isomer of catechol, in which the neighboring hydroxyl groups will lead to the coupling of anionic forms,<sup>[10]</sup>  $H_2BQ$  possesses a reversible two-electron-transfer reaction in water.<sup>[5a]</sup> With the help of rotating disk electrode (RDE) and cyclic voltammetry (CV) measurements, the redox chemistry of  $H_2BQ$  is investigated in a broad pH range. By tuning the concentration of protons, both the reaction process and the redox potential can be manipulated. In slightly basic environment, the solubility of  $H_2BQ$  can reach more than 1 M in water, which corresponds to 2 Faraday of charge per liter in the two-electron-involved reaction. The demonstrated energy density can reach  $60 \text{ Wh L}^{-1}$ , which is comparable or better than recent reports about liquid batteries.<sup>[2,11]</sup> Distinguished from other complex quinone structures investigated before, its natural occurrences and mature industrial production as small molecule make  $H_2BQ$  appealing for commercial applications.<sup>[12]</sup> On the other hand, as a discharged state of cathode-active species,  $H_2BQ$  can be coupled with graphite to build a full battery. Therefore, limitations including high cost of production, low output potential and dendrites issues faced in previous researches can be circumvented. All these features promise one novel type of green energy storage system.

The working principle of this liquid battery is illustrated in Figure 1, in which the anode reaction is based on the

[\*] Y. Ding, Prof. G. Yu  
Materials Science and Engineering Program and  
Department of Mechanical Engineering  
The University of Texas at Austin  
Austin, TX 78712 (USA)  
E-mail: ghyu@austin.utexas.edu

Supporting information for this article can be found under <http://dx.doi.org/10.1002/anie.201600705>.

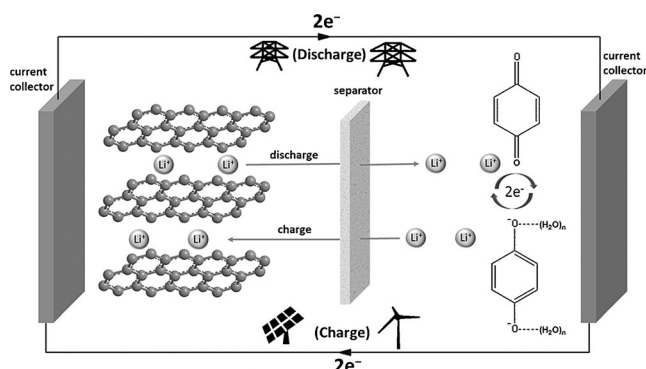


**Figure 1.** Working principle of the designed liquid battery with H<sub>2</sub>BQ aqueous solution as catholyte and graphite in aprotic electrolyte as anode. The direction of Li<sup>+</sup> diffusion inside battery and electron transference in external circuit indicates charge or discharge mode, and curved arrows indicate the direction of the redox reaction in the cathode part. The cartoon on top shows that in discharge mode the battery can provide energy through an electrical grid, and the cartoon below shows sustainable energy sources from wind and sun in charge mode.

intercalation and de-intercalation process of Li ions in graphite, and the cathode part is based on the redox reaction of H<sub>2</sub>BQ with the transference of Li ions to balance the charge. As for the separator, a NASICON type Li-ion-conducting solid membrane LTP (Li<sub>1+x+3z</sub>Al<sub>x</sub>(Ti,Ge)<sub>2-3x</sub>Si<sub>3z</sub>P<sub>3-2z</sub>O<sub>12</sub>) functions to transfer Li ions and restrict crossover of redox species and electrolyte. Given two hydroxy groups in H<sub>2</sub>BQ are bonded to the aromatic ring in a *para* position, the feasibility of the redox reaction should be related to the reorganization of the conjugated double bond. RDE test was firstly carried out to explore the electrochemistry of H<sub>2</sub>BQ (Figure 2). In the potential range between 0.2 V and 1.1 V (vs. SHE), a flat limiting current plateau corresponds to

a one-step two-electron-transfer reaction, which correlates well with published literature.<sup>[5a,9a]</sup> The redox potential of H<sub>2</sub>BQ can also be estimated from the half-wave potential, which is about 0.6 V and this value is comparable with iodine/iodide,<sup>[3c]</sup> but the abundance and environmental-friendliness of H<sub>2</sub>BQ are more prominent. RDE measurement at different rates yields limiting current controlled by mass transport, from which the diffusion coefficient (*D*) of H<sub>2</sub>BQ can be obtained using Levich equation:<sup>[13]</sup>

$$i_{\text{lim}} = 0.62nFAD^{2/3}\omega^{1/2}\nu^{-1/6}C \quad (1)$$

in which *i*<sub>lim</sub> is limiting current, *n* is the number of electrons transferred, *F* is Faraday constant, *A* is the surface area of electrode,  $\omega$  is angular rotation rate,  $\nu$  is the kinetic viscosity, *C* is the bulk concentration. The calculated *D* ( $8.8 \times 10^{-6} \text{ cm}^2 \text{ s}^{-1}$ ) is similar to those of redox couples in aqueous flow batteries, but several orders of magnitude larger than that of Li ion in solid state Li-ion batteries.<sup>[2b]</sup> Koutecky-Levich analysis indicates that the redox reaction is controlled by both diffusion and kinetic effect, and the kinetic current *i*<sub>k</sub> without mass transport limitation can be obtained by extrapolating rotation rate to infinity according to Koutecky-Levich equation (Eq. (2); Figure 2c).<sup>[13]</sup>

$$\frac{1}{i} = \frac{1}{i_k} + \frac{1}{0.62nFAD^{2/3}\omega^{1/2}\nu^{-1/6}C} \quad (2)$$

The exchange current (*i*<sub>0</sub>) can be obtained by fitting Butler-Volmer equation at overpotential of zero (Figure 2d), and the reaction rate constant (*k*<sub>0</sub>) was calculated to be  $2.0 \times 10^{-3} \text{ cm s}^{-1}$  according to Equation (3).

$$i_0 = nFACk_0 \quad (3)$$

This rate constant is larger than most of the redox species in commercial redox flow batteries,<sup>[1b]</sup> such as VO<sub>2</sub><sup>+</sup>/VO<sup>2+</sup>, Fe<sup>3+</sup>/Fe<sup>2+</sup> and Br<sub>2</sub>/Br<sup>−</sup> (Table S1), implying that voltage loss due to activation polarization of H<sub>2</sub>BQ-based liquid battery is mitigated greatly. In light of the structure of H<sub>2</sub>BQ molecule, the high rate should be attributed to the outer-sphere electron-transfer process, with small energy needed to reorganize the aromatic  $\pi$ -orbital system.<sup>[9a]</sup>

To gain a better understanding of the electrochemistry of H<sub>2</sub>BQ, CV tests were conducted in a broad pH range between 1 and 9 (see Figure S2 in the Supporting Information). The pH-dependence of CV curves is shown in Figure 3a and increasing pH can shift the potential of the proton-involved reaction to more negative values. But when the concentration of proton is reduced greatly, the redox potential becomes pH-independent. This trend can be explained clearly by manipulating Nernst equation of the redox reaction [Eqs. (4) and (5)].



$$E = E^\circ - \frac{RT}{nF} \ln \frac{[\text{H}_m\text{BQ}^{m-n}]}{[\text{BQ}][\text{H}^+]^m} \quad (5)$$

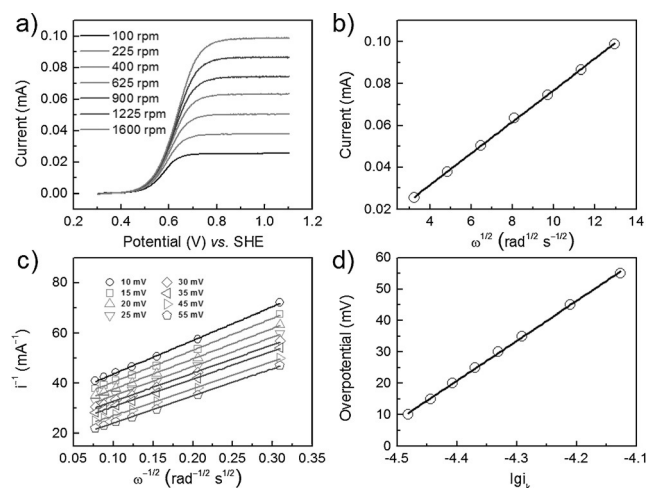


**Figure 2.** a) RDE measurements of 1 mM H<sub>2</sub>BQ in 0.2 M Li<sub>2</sub>SO<sub>4</sub> solution at rotation rates from 100 rpm to 1600 rpm with a scan rate of 5 mV s<sup>−1</sup> on a glassy carbon electrode. b) Levich plot of limiting current versus square root of rotation rates ( $\omega^{1/2}$ ). c) Koutecky-Levich plots derived from different overpotentials. d) Fit of Butler-Volmer equation derived from (c) at different overpotentials.

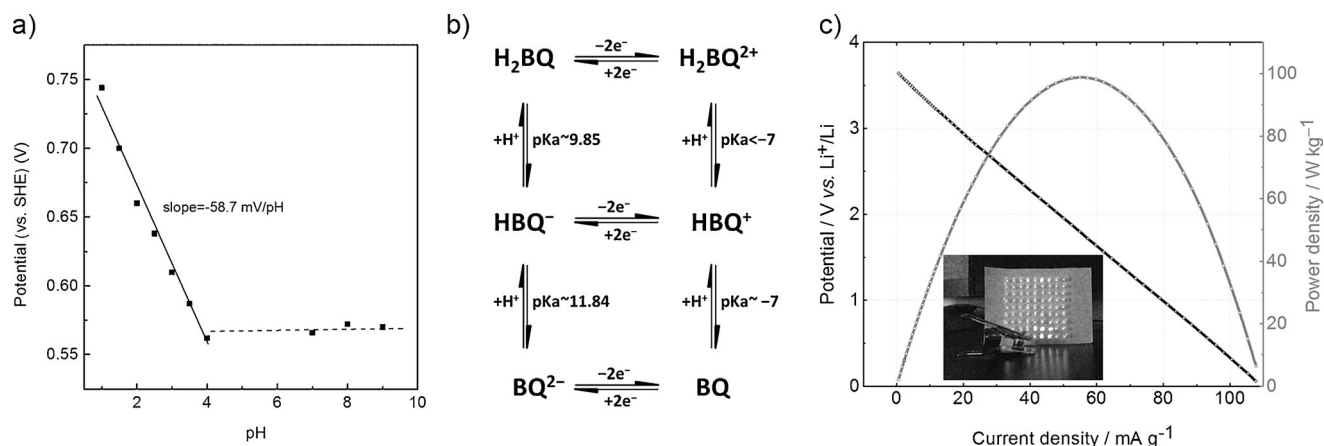


**Figure 3.** a) Potential ( $E_{1/2}$ ) versus pH value for 1 mM H<sub>2</sub>BQ in 0.2 M Li<sub>2</sub>SO<sub>4</sub> solution at scan rate of 25 mV s<sup>-1</sup>. b) Redox reaction and proton-transfer reactions of H<sub>2</sub>BQ. c) Polarization curve of the full liquid cell and the inserted picture shows the demo to power 81 LED bulbs.

The redox potential for an  $mH^+$ ,  $ne^-$  involved reaction should change  $-(m/n)59$  mV/pH at temperature of 25 °C. In the pH range of 1–4, the reduced species is in the fully protonated state, thus it undergoes a  $2H^+$ ,  $2e^-$  process and the theoretical slope should be  $-59$  mV/pH, corresponding well with the experimentally fitted value of  $-58.7$  mV/pH in Figure 3a. When the concentration of protons decreases greatly, the reduced species may exist in the form of deprotonated state, and the redox potential will be pH independent, as illustrated in the region of pH above 7 (Figure 3a). This result agrees with published reports,<sup>[5a]</sup> and we can further summarize the possible redox reaction and proton-transfer process of H<sub>2</sub>BQ in Figure 3b. This is a two-electron-transfer reaction, but the reduced species may be a mixture of BQ<sup>2-</sup>, protonated anion HBQ<sup>-</sup> and hydroquinone H<sub>2</sub>BQ with different distributions at different pH values. In acidic environment, most of the distribution will be fully protonated H<sub>2</sub>BQ, thus breaking of O–H bond in the redox reaction process should require more activation energy. While in basic condition, the constituent will mainly contain anion BQ<sup>2-</sup>, of which the redox reaction is less complex and the redox potential is pH-independent. As a result, to maximize the solubility of redox species, decrease the complexity of the redox reaction, and maintain the stability of solid electrolyte, we tune the pH value to 9 by adding LiOH solution. With H<sub>2</sub>BQ in weak basic environment as catholyte, the reduced state can couple with graphite anode to construct a full cell. Polarization curve in Figure 3c exhibits the potential–current and power–current response. The maximum power density of the full cell can reach about 100 W kg<sup>-1</sup> based on the total weight of catholyte solution at current density of 58 mA g<sup>-1</sup> at room temperature. This power density is comparable to that of other reported redox flow batteries<sup>[3d]</sup> and can be improved further by exploiting advanced solid electrolyte in view of the fast kinetics and diffusion coefficient of H<sub>2</sub>BQ.<sup>[14]</sup> The inset in Figure 3c showing that one liquid cell lights a 9 × 9 LED bulb array also shows the good electrochemical performance.

To further test the feasibility of H<sub>2</sub>BQ-based liquid battery, the catholyte was subjected to electrochemical measurements in a half cell format using Li anode. In this

study, a home-made cell was adopted to demonstrate the performance, which is composed of a cathode part with titanium foil coated with activated carbon as current collector, H<sub>2</sub>BQ and Li salt in water as catholyte, a NASICON-type LATP membrane as separator, and Li metal as anode. The detailed device assembly process was introduced in Supporting Information. Galvanostatic charge/discharge measurement at 0.4 C (1 C = 487 mA g<sup>-1</sup>) was first conducted, and Figure S3 shows the initial specific charge capacity of 456 mAh g<sup>-1</sup> with Coulombic efficiency (CE) of 89% and working potential about 3.5 V. This demonstrates that 93% of theoretical capacity (487 mAh g<sup>-1</sup>) can be used. Given the fast reaction kinetics and large diffusion coefficient of H<sub>2</sub>BQ, the untapped capacity should be largely because of limited Li ion conductivity of the Li ion membrane (ca.  $10^{-4}$  S cm<sup>-1</sup> at room temperature).<sup>[2b]</sup> The specific capacity is among the highest values in recent reports,<sup>[2b]</sup> benefited from the small molecular structure and efficient two-electron-transfer reaction. Figure S4 presents that the discharge capacity was stable with decay as little as 0.3% per cycle, and the CE was stabilized to nearly 100% since the second cycle. Additionally, stabilized voltage efficiency (VE) and energy efficiency (EE) can maintain about 93% and 92% as shown in Figure S5. Such small voltage loss can be attributed to the fast outer-sphere electron-transfer process demonstrated by RDE before.

As explored above, the reaction process is strongly affected by the concentration of protons in catholyte, and we also tested the half cell at the pH value of 2 (Figure S6). The capacity degrades greatly, and the hysteresis becomes more serious, thus smaller proton concentration is preferred in our system, and we set the pH value of 9 to avoid corrosion of LATP separator in strong basic environment. As the energy density of liquid battery is not only proportional to the number of electrons transferred and working potential of the redox species, but also dependent on its solubility, next we tested the battery at different concentrations. Figure S7 shows that the volumetric capacity can reach above 17 Ah L<sup>-1</sup>, which corresponds to energy density of 60 Wh L<sup>-1</sup>. This value is comparable or better than current energy-storage technologies of liquid-form electrodes (Figure S8).<sup>[2b]</sup>



Based on these results, a heavy-metal-free liquid battery was built using  $\text{H}_2\text{BQ}$  solution as cathode-active part and graphite as anode. As a proof-of-concept system, a similar cell structure was designed as the half-cell, with the only change being that graphite suspension is casted on copper mesh as anode. The discharge potential of the full cell maintains at 3.4 V, as shown in the voltage profile (Figure 4b), which is

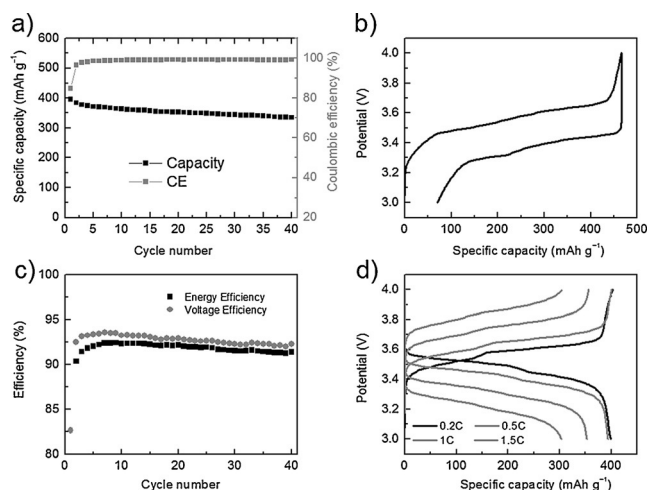


**Figure 4.** a) Cycling performance of the full cell at 0.4 C. b) Charge–discharge curve for the first cycle. c) Corresponding energy and voltage efficiency. d) Rate performance of the full cell.

much larger than conventional aqueous flow batteries restricted by the electrolysis of water (1.23 V). This result also correlates well with half-cell data, in which the discharge potential of  $\text{H}_2\text{BQ}$  maintains about 3.5 V and the charge potential of graphite is about 0.1 V.<sup>[15]</sup> In such a full cell, crossover of active species can be limited to the minimum extent confirmed by the stabilized CE of over 99%. In the cycling test, the stabilized VE is about 93% and EE is about 92%, both of which greatly exceed those of the reported non-aqueous flow batteries (EE ca. 20–50%).<sup>[16]</sup> Cycling performance in Figure 4a shows about 99.7% retention per cycle, which is similar to that of the half cell in Figure S4. The nearly overlapped voltage profiles over time in Figure S9 indicate excellent stability of the  $\text{H}_2\text{BQ}$  redox species during the electrochemical process. Rate performance in Figure 4d indicates that 98.7%, 88.6% and 76.1% of the capacity can be retained when the tested current rates changed from 0.2 C to 0.5 C, 1 C and 1.5 C with CE at all rates maintaining nearly 100%. The untapped capacity at high rates is attributed to the ohmic polarization of solid electrolyte, and the rate capability can be further enhanced with development of advanced Li-ion conductors.<sup>[14]</sup> The excellent rate performance is in accordance with the high power density shown in polarization curve. Long-term stability of this full cell was also examined. XRD patterns and SEM images of pristine separator and the one after 40 cycles show almost the same crystalline structure and porous morphology (Figure S10,S11), indicating the good stability of LATP in the weak basic environment.

Inspired by the pivotal role of quinones in nature, we design a heavy-metal-free, dual-electrolyte liquid battery. By directly using  $\text{H}_2\text{BQ}$  in water as catholyte and graphite as anode, specific discharge capacity of  $395 \text{ mAh g}^{-1}$  is obtained with the working potential of 3.4 V. As one of the simplest forms of organic redox species,  $\text{H}_2\text{BQ}$  can be extracted directly from living organisms, and the outer-sphere electron-transfer reaction with small activation energy to reorganize the aromatic  $\pi$  bond contributes to high reaction rate constant, therefore all these features promise a cost-effective energy storage system that may output superior performance without environmental disturbance. As the development of flow batteries relies on the development of redox-active materials, quinone-represented organic redox species provide much freedom to design metal-free batteries toward sustainable energy storage. The tunable properties can be realized by electrolyte solvent selection. Additionally the structure diversity of organic materials allows the tailoring of solubility, electrochemical activity and redox potential by functionalization with certain groups.<sup>[2b]</sup> For example, when the concentration of  $\text{H}_2\text{BQ}$  reaches more than 0.5 M, CE for the first cycle drops obviously due to low solubility of BQ, and this concern can be alleviated by functionalizing  $\text{H}_2\text{BQ}$  with hydrophilic groups such as sulfonic group to improve solubility, so as to expect higher energy density. Nowadays the performance of metal-free flow battery is limited in the anode part, and selection of organic anode-active materials with low potential can lead to the construction of high-performance all-organic flow batteries. Moreover, the graphite anode can even be replaced with anode suspensions like Si, which may stretch the research boundaries of different kinds of batteries, and broaden the extent of novel energy storage devices with new chemistry.<sup>[17]</sup> By designing such a battery mainly using C, H and O as building blocks to fabricate redox species, the rapid growth and moving frontiers of atom economy in green chemistry can be extended to the field of energy storage. Thus this new-concept battery is promising to meet the system capital cost target of \$150 per kWh set by US Department of Energy.

## Acknowledgements

G.Y. acknowledges the financial support from the National Science Foundation award (grant number NSF-CMMI-1537894) and 3M Nontenured Faculty Award.

**Keywords:** electrochemistry · liquid batteries · metal-free · quinone · sustainable chemistry

**How to cite:** *Angew. Chem. Int. Ed.* **2016**, *55*, 4772–4776  
*Angew. Chem.* **2016**, *128*, 4850–4854

- [1] a) M. H. Chakrabarti, R. A. W. Dryfe, E. P. L. Roberts, *Electrochim. Acta* **2007**, *52*, 2189–2195; b) A. Weber, M. Mench, J. Meyers, P. Ross, J. Gostick, Q. Liu, *J. Appl. Electrochem.* **2011**, *41*, 1137–1164; c) K. Gong, X. Ma, K. M. Conforti, K. J. Kuttler, J. B. Grunewald, K. L. Yeager, M. Z. Bazant, S. Gu, Y. Yan, *Energy Environ. Sci.* **2015**, *8*, 2941–2945.

- [2] a) Y. Wang, P. He, H. Zhou, *Adv. Energy Mater.* **2012**, 2, 770–779; b) Y. Zhao, Y. Ding, Y. Li, L. Peng, H. R. Byon, J. B. Goodenough, G. Yu, *Chem. Soc. Rev.* **2015**, 44, 7968–7996.
- [3] a) Y. Wang, Y. Wang, H. Zhou, *ChemSusChem* **2011**, 4, 1087–1090; b) Y. Lu, J. B. Goodenough, Y. Kim, *J. Am. Chem. Soc.* **2011**, 133, 5756–5759; c) Y. Zhao, L. Wang, H. R. Byon, *Nat. Commun.* **2013**, 4, 1896–1902; d) Y. Zhao, Y. Ding, J. Song, G. Li, G. Dong, J. B. Goodenough, G. Yu, *Angew. Chem. Int. Ed.* **2014**, 53, 11036–11040; *Angew. Chem.* **2014**, 126, 11216–11220; e) Y. Zhao, Y. Ding, J. Song, L. Peng, J. B. Goodenough, G. Yu, *Energy Environ. Sci.* **2014**, 7, 1990–1995; f) Y. Ding, Y. Zhao, G. Yu, *Nano Lett.* **2015**, 15, 4108–4113; g) Y. Zhao, H. R. Byon, *Adv. Energy Mater.* **2013**, 3, 1630–1635; h) L. Wang, Y. Zhao, M. L. Thomas, A. Dutta, H. R. Byon, *ChemElectroChem* **2015**, DOI: 10.1002/celec.201500342; i) K. Takechi, Y. Kato, Y. Hase, *Adv. Mater.* **2015**, 27, 2501–2506; j) C. Jia, F. Pan, Y. G. Zhu, Q. Huang, L. Lu, Q. Wang, *Sci. Adv.* **2015**, DOI: 10.1126/sciadv.1500886.
- [4] a) C. S. Sevov, R. E. M. Brooner, E. Chenard, R. S. Assary, J. S. Moore, J. Rodriguez-Lopez, M. S. Sanford, *J. Am. Chem. Soc.* **2015**, 137, 14465–14472; b) D. Larcher, J. M. Tarascon, *Nat. Chem.* **2015**, 7, 19–29.
- [5] a) M. Quan, D. Sanchez, M. F. Wasylkiw, D. K. Smith, *J. Am. Chem. Soc.* **2007**, 129, 12847–12856; b) D. T. Scott, D. M. McKnight, E. L. Blunt-Harris, S. E. Kolesar, D. R. Lovley, *Environ. Sci. Technol.* **1998**, 32, 2984–2989; c) H. Kurreck, M. Huber, *Angew. Chem. Int. Ed. Engl.* **1995**, 34, 849–866; *Angew. Chem.* **1995**, 107, 929–947.
- [6] a) M. Lee, J. Hong, H. Kim, H. D. Lim, S. B. Cho, K. Kang, C. B. Park, *Adv. Mater.* **2014**, 26, 2558–2565; b) M. Park, D. S. Shin, J. Ryu, M. Choi, N. Park, S. Y. Hong, J. Cho, *Adv. Mater.* **2015**, 27, 5141–5146; c) H. Wang, P. Hu, J. Yang, G. Gong, L. Guo, X. Chen, *Adv. Mater.* **2015**, 27, 2348–2354.
- [7] M. Yao, H. Senoh, S. Yamazaki, Z. Siroma, T. Sakai, K. Yasuda, *J. Power Sources* **2010**, 195, 8336–8340.
- [8] K. Lin, Q. Chen, M. R. Gerhardt, L. Tong, S. B. Kim, L. Eisenach, A. W. Valle, D. Hardee, R. G. Gordon, M. J. Aziz, M. P. Marshak, *Science* **2015**, 349, 1529–1532.
- [9] a) B. Huskinson, M. P. Marshak, C. Suh, S. Er, M. R. Gerhardt, C. J. Galvin, X. Chen, A. Aspuru-Guzik, R. G. Gordon, M. J. Aziz, *Nature* **2014**, 505, 195–198; b) S. Nawar, B. Huskinson, M. Aziz, *MRS Proc.* **2013**, DOI: 10.1557/opl.2012.1737; c) W. Wang, W. Xu, L. Cosimbescu, D. Choi, L. Li, Z. Yang, *Chem. Commun.* **2012**, 48, 6669–6671; d) H. Senoh, M. Yao, H. Sakaebe, K. Yasuda, Z. Siroma, *Electrochim. Acta* **2011**, 56, 10145–10150.
- [10] D. Nematollahi, M. Rafiee, *J. Electroanal. Chem.* **2004**, 566, 31–37.
- [11] a) F. R. Brushett, J. T. Vaughey, A. N. Jansen, *Adv. Energy Mater.* **2012**, 2, 1390–1396; b) X. Wei, W. Xu, J. Huang, L. Zhang, E. Walter, C. Lawrence, M. Vijayakumar, W. A. Henderson, T. Liu, L. Cosimbescu, B. Li, V. Sprenkle, W. Wang, *Angew. Chem. Int. Ed.* **2015**, 54, 8684–8687; *Angew. Chem.* **2015**, 127, 8808–8811.
- [12] G. A. Burdock, *Food Chem. Toxicol.* **1998**, 36, 347–363.
- [13] A. J. Bard, L. R. Faulkner, *Electrochemical Methods: Fundamentals and Applications*, 2nd ed., Wiley, Hoboken, **2001**.
- [14] Z. Liu, W. Fu, E. A. Payzant, X. Yu, Z. Wu, N. J. Dudney, J. Kiggans, K. Hong, A. J. Rondinone, C. Liang, *J. Am. Chem. Soc.* **2013**, 135, 975–978.
- [15] J.-i. Yamaki, H. Takatsuji, T. Kawamura, M. Egashira, *Solid State Ionics* **2002**, 148, 241–245.
- [16] S.-H. Shin, S.-H. Yun, S.-H. Moon, *RSC Adv.* **2013**, 3, 9095–9116.
- [17] S. Hamelet, D. Larcher, L. Dupont, J. M. Tarascon, *J. Electrochem. Soc.* **2013**, 160, A516–A520.

Received: January 21, 2016

Revised: February 9, 2016

Published online: March 9, 2016